DOI: 10.1534/genetics.107.072413

SYP-3 Restricts Synaptonemal Complex Assembly to Bridge Paired Chromosome Axes During Meiosis in *Caenorhabditis elegans*

Sarit Smolikov,* Andreas Eizinger,* Kristina Schild-Prufert,* Allison Hurlburt,* Kent McDonald,† JoAnne Engebrecht,‡,[1] Anne M. Villeneuve‡ and Mónica P. Colaiácovo*,[2]

**Department of Genetics, Harvard Medical School, Boston, Massachusetts 02115, †Electron Microscope Laboratory, University of California, Berkeley, California 94720 and ‡Departments of Developmental Biology and Genetics, Stanford University School of Medicine, Stanford, California 94305*

Manuscript received February 20, 2007
Accepted for publication May 31, 2007

ABSTRACT

Synaptonemal complex (SC) formation must be regulated to occur only between aligned pairs of homologous chromosomes, ultimately ensuring proper chromosome segregation in meiosis. Here we identify SYP-3, a coiled-coil protein that is required for assembly of the central region of the SC and for restricting its loading to occur only in an appropriate context, forming structures that bridge the axes of paired meiotic chromosomes in *Caenorhabditis elegans*. We find that inappropriate loading of central region proteins interferes with homolog pairing, likely by triggering a premature change in chromosome configuration during early prophase that terminates the search for homologs. As a result, *syp-3* mutants lack chiasmata and exhibit increased chromosome missegregation. Altogether, our studies lead us to propose that SYP-3 regulates synapsis along chromosomes, contributing to meiotic progression in early prophase.

SEXUALLY reproducing organisms must reduce their chromosome number by half to generate haploid gametes. This is accomplished through meiosis, a specialized form of cell division, composed of meiosis I (a reductional division) and meiosis II (an equational division). A series of discrete steps unfold during prophase of meiosis I, ultimately ensuring proper chromosome segregation (Zickler and Kleckner 1999; Page and Hawley 2003). In particular, homologous chromosomes pair, and a zipper-like proteinaceous structure known as the synaptonemal complex (SC) assembles between paired and aligned homologs. In parallel, meiotic recombination initiates with the formation of double-strand breaks (DSBs), a subset of which is subsequently repaired as crossovers. Upon progression into late prophase, the SC disassembles but homologs remain attached to each other via chiasmata imparted by those earlier crossover events in collaboration with sister chromatid cohesion. These physical connections between homologous chromosomes are crucial for their proper orientation at the metaphase I plate and consequent disjunction to opposite poles of the spindle.

Superimposed onto the processes of pairing, synapsis, and recombination is the dynamic nuclear reorganization that is undergone by chromosomes during meiotic prophase. Upon entrance into meiosis (leptotene/zygotene), chromosomes acquire a polarized spatial organization within the nucleus. This can involve either the attachment of telomeres to the inner nuclear envelope and their subsequent clustering leading to the formation of a chromosomal "bouquet" within a nuclear subdomain or the clustering of chromosomes toward one side of the nucleus without a clustering of telomeres (Zickler and Kleckner 1998; Scherthan 2001; Harper *et al.* 2004; Gerton and Hawley 2005). Chromosomes then exit this clustered organization and redisperse throughout the nuclear periphery (pachytene) concomitantly with the completion of synapsis.

Studies of several mutants in budding yeast, fission yeast, maize, and worms, where either telomere clustering is defective or chromosomes fail to cluster upon meiotic entry, indicate that acquisition of a polarized spatial organization by chromosomes is implicated in the proper timing or efficacy of homologous pairing (Chua and Roeder 1997; Conrad *et al.* 1997; Cooper *et al.* 1998; Nimmo *et al.* 1998; Trelles-Sticken *et al.* 2000; MacQueen and Villeneuve 2001; Golubovskaya *et al.* 2002; Couteau *et al.* 2004; Ding *et al.* 2004; Nabeshima *et al.* 2004). Recent studies suggest that both acquisition of a clustered organization by chromosomes and homologous pairing are actively promoted processes. In fission yeast, a protein complex involving Bqt1 and Bqt2 connects telomeric ends and the spindle pole body and actively drives chromosomes into the bouquet configuration in response to mating pheromone (Chikashige *et al.* 2006). In *Caenorhabditis elegans*, a genetically defined

[1]*Present address:* Section of Molecular and Cellular Biology, University of California, Davis, CA 95616.

[2]*Corresponding author:* Department of Genetics, Harvard Medical School, 77 Avenue Louis Pasteur, NRB-334, Boston, MA 02115. E-mail: mcolaiacovo@genetics.med.harvard.edu

cis-acting region known as the pairing center (PC) located at one end of every chromosome has been previously implicated in promoting stable homologous pairing (McKim *et al.* 1988; Villeneuve 1994; MacQueen *et al.* 2002, 2005). The recent identification of a family of C2H2 zinc-finger proteins that specifically binds at the PC regions of chromosomes and associates with the nuclear envelope also suggests that homologous pairing is actively promoted in *C. elegans* (Phillips *et al.* 2005; Phillips and Dernburg 2006).

However, while both the mechanism and proteins driving chromosomes into this polarized nuclear organization are starting to be understood, not much is known about how chromosomes are driven out of this configuration in later stages of meiosis. Studies in budding yeast and mice suggest that this is an actively regulated process possibly involving recombination checkpoints, given that the initiation and progression of meiotic recombination are required for chromosome redispersal (Pandita *et al.* 1999; Trelles-Sticken *et al.* 1999; Scherthan *et al.* 2000). However, both in *Drosophila melanogaster* and in *C. elegans*, chromosomes successfully redisperse and are fully synapsed in pachytene without the initiation of meiotic recombination (Dernburg *et al.* 1998; McKim *et al.* 1998). The recent analysis of HTP-1, a HORMA-domain protein that inhibits nonhomologous synapsis and is implicated in the coordination between pairing and synapsis, suggests that exit from a clustered organization is an actively regulated process in *C. elegans* (Couteau and Zetka 2005; Martinez-Perez and Villeneuve 2005). However, how the relay between progression of pairing and SC formation occurs and to what degree structural components of the SC are involved in this process remains unclear.

The SC is a tripartite structure observed continuously along the full length between paired and aligned homologous chromosomes. It consists of proteins associated along the axis of each homolog, comprising the two lateral elements of the SC, flanking a central region containing transverse filament proteins. Axis-associated components consist of cohesin and condensin proteins along with noncohesin structural components of the lateral elements. Proteins forming the transverse filaments are structural modules of the SC consisting of an extended coiled-coil domain flanked by globular domains (Page and Hawley 2004; Colaiácovo 2006).

The identification and functional analysis of SC components in *C. elegans* is playing an integral role in revealing how events such as pairing, synapsis, and recombination interface to drive meiotic progression (Colaiácovo 2006). For instance, HIM-3 is a lateral element component of the SC in *C. elegans* and a homolog of Hop1, a lateral element protein in *Saccharomyces cerevisiae*. Studies of *him-3* mutants revealed that while initiation of recombination can proceed despite defective axis morphogenesis, homologous pairing, chromosome synapsis, and chiasma formation are impaired (Zetka *et al.* 1999; Couteau *et al.* 2004). Whereas, SYP-1 and SYP-2 are central region components of the SC in *C. elegans*, and analysis of *syp-1* and *syp-2* mutants revealed that synapsis is required for the stabilization of initial homologous pairing interactions and the consequent formation of chiasmata (MacQueen *et al.* 2002; Colaiácovo *et al.* 2003). Moreover, the analysis of *syp-1* and *syp-2* mutants suggested that the establishment of pairing and local stabilization of pairing at the PC regions occurred independently from the SC (MacQueen *et al.* 2002; Colaiácovo *et al.* 2003).

In this study, we identify SYP-3, a new structural component of the SC. Our studies show that SYP-3 is required for assembly of the SC central region and for restricting loading of central region proteins to occur only in an appropriate context, forming structures that bridge the axes of paired meiotic chromosomes. SYP-3 is also required for the stabilization of homologous chromosome pairing and chiasma formation due to its requirement for the timely and appropriate assembly of the SC between homologs. Moreover, our analysis of *syp-3* mutants supports a model in which progression of synapsis serves as a trigger leading chromosomes to exit a polarized configuration and redisperse throughout the nuclear periphery during early prophase. Altogether, our analysis of *syp-3* mutants reveals how changes in both chromosome organization and structural constraints throughout prophase interface with the processes of pairing and synapsis.

MATERIALS AND METHODS

Genetics: *C. elegans* strains were cultured at 20° under standard conditions as described in Brenner (1974). Bristol N2 worms were utilized as the wild-type background. Hawaiian CB4856 wild-type worms were utilized only for SNP mapping (Wicks *et al.* 2001). The following mutations and chromosome rearrangements were used (Riddle *et al.* 1997; MacQueen *et al.* 2002; Colaiácovo *et al.* 2003; Couteau *et al.* 2004; Martinez-Perez and Villeneuve 2005; this work):

LGI: *syp-3(me42, ok758), hT2[bli-4(e937) qIs48] (I;III), nDf23, dpy-5(e61), unc-75(e950)*
LGIV: *htp-1(me84), him-3(gk149)*
LGV: *syp-2(ok307), syp-1(me17)*

syp-3(me42) was isolated following EMS mutagenesis as in Kelly *et al.* (2000) and was localized by three-factor crosses and SNP mapping (Wicks *et al.* 2001) to within 0.5 cM of pkP1059, located 17 kb from F39H2.4 on chromosome I. The *syp-3(ok758)* deletion allele was generated by the *C. elegans* Gene Knockout Consortium. In parallel, F39H2.4 was identified through a functional genomics approach applied to the identification of meiotic genes (Colaiácovo *et al.* 2002) and was located in the interval to which *syp-3* was mapped. This gene had increased expression in the germline (Reinke *et al.* 2000) and upon depletion via RNAi elicited meiotic defects similar to that of *syp-3(ok758)*. Sequence analysis indicated that *syp-3(me42)* mutant worms carry a nonsense mutation in the F39H2.4 coding region, resulting in a stop codon at position 214 of the 224-amino acid protein.

Gene structure: First-strand cDNA corresponding to F39H2.4 was generated by reverse-transcription of adult poly(A) RNA,

using reverse primer: 5′-CCGAACTGTGTACCCGCACT-3′. This cDNA pool was used as template in PCR reactions to amplify distinct regions of the F39H2.4 predicted transcript. PCR products generated by 5′ RACE or using SL1 forward primers were sequenced. This analysis revealed a revised gene structure encoding a protein with an additional 40 amino acids upstream of the N-terminus prediction in WormBase release WS162.

Characterization of alleles: Both *syp-3(me42)* and *syp-3(ok758)* exhibit weak semidominant effects. Low levels of embryonic lethality and a very mild *h*igh *i*ncidence of *m*ales (Him) phenotype are observed among the progeny of *syp-3(me42)/+* (12.8% embryonic lethality and 3.4% male progeny; $n = 1414$) and *syp-3(ok758)/+* (8% embryonic lethality and 1% male progeny; $n = 1589$) hermaphrodites. This is accompanied by a low frequency of univalents (seven as opposed to six DAPI-staining bodies) observed in diakinesis oocytes for *syp-3(me42)/+* (17%; $n = 30$) and *syp-3(ok758)/+* (13%; $n = 30$). No other changes in either the temporal progression or DAPI morphology of chromosomes were observed in these heterozygotes throughout meiotic prophase.

DAPI-stained germlines of *trans*-heterozygotes for *me42* and *nDf23* or *ok758* and *nDf23* were indistinguishable from either *me42* or *ok758* homozygotes, respectively. The most severe *syp-3(RNAi)* chromosome morphology observed revealed identical defects to those observed in *syp-3(ok758)*. Moreover, SYP-3 immunolocalization onto chromosomes is no longer observed in *syp-3(ok758)* mutants when using either the α-SYP-3 N-terminal or C-terminal antibodies, while it is observed in *syp-3(me42)* mutants when using either antibody (the α-SYP-3 C-terminal antibody was raised using a peptide sequence located mostly upstream of the premature stop codon identified in this mutant; see below). Taken together, these results indicate *syp-3(ok758)* is a null and that its semidominance effects result from haplo-insufficiency. Similar semidominance effects are observed among the progeny of *syp-2(ok307)/+* (R. Yokoo and A. Villeneuve, personal communication), suggesting that haploinsufficiency may be a shared feature among mutants of structural components of the SC.

Antibody preparation, DAPI analysis, and immunostaining: Rabbit α-SYP-3 N-terminal and C-terminal polyclonal antibodies were generated using peptide antigens corresponding, respectively, to MRQIETQQLEAETSFTERIA and IFHYQVAKLRSEYQKCRLQE (generated by Biosynthesis). Animals were immunized and bled by Covance Research Products. SYP-3 is not detected on chromosomes *in situ* on *syp-3(ok758)* mutants when using either the α-SYP-3 C-terminal or α-SYP-3 N-terminal antibodies, indicating that these antibodies are specific to SYP-3. All experiments were performed without further purification of the SYP-3 antisera. We have subsequently determined that its purification does not alter any of the staining patterns reported here. Analysis of SYP-3 protein on Westerns has not been possible so far given that neither these antisera nor those we attempted to generate through additional strategies recognize SYP-3 on Westerns.

DAPI staining, immunostaining, and analysis of stained meiotic nuclei were carried out as in Colaiácovo *et al.* (2003), except for α-REC-8 staining, which was performed as in Rogers *et al.* (2002). Antibodies were used at the following dilutions: α-SYP-1 (1:200), α-SYP-2 (1:100), α-SYP-3 (1:100), α-HIM-3 (1:100), α-HTP-3 (1:500), and α-REC-8 (1:100). Double-labeling experiments were performed as in Colaiácovo *et al.* (2003). Secondary antibodies used were: FITC or Cy3 anti-rabbit and Cy3 anti-guinea pig (Jackson Immunochemicals), each at 1:200; Alexa 488 anti-guinea pig and Alexa 488 anti-mouse (Molecular Probes, Eugene, OR), each at 1:400.

Fluorescence *in situ* hybridization and time-course analysis of chromosome pairing: 5S rDNA probe, X left end probe derived from YAC Y51E2, X right end probe derived from YAC Y68A3, chromosome I left end probe derived from pooled cosmids D1037, ZC535, F21A9, and chromosome I right end probe derived from pooled cosmids F32A7 and F14B11 were generated and labeled as in Dernburg *et al.* (1998) and Zalevsky *et al.* (1999). Homologous pairing was monitored quantitatively as in MacQueen and Villeneuve (2001), with fluorescence *in situ* hybridization (FISH) signals considered paired when separated by ≤0.75 μm. The average numbers of nuclei scored per zone (n) with all probes for wild-type, *syp-2*, *syp-3(ok758)*, and *syp-3(me42)* are as follows: zone 1 ($n = 101$), zone 2 ($n = 105$), zone 3 ($n = 104$), zone 4 ($n = 94$), zone 5 ($n = 99$), zone 6 ($n = 94$), and zone 7 ($n = 86$). Between 65 and 85 nuclei were scored per zone for *syp-1* and *syp-3(me42); syp-1*, with 5S rDNA and chromosome I right end probes.

RNA interference: Production of double-stranded RNA for *rec-8(RNAi)* and the RNAi procedure were carried out as described in Colaiácovo *et al.* (2003).

Electron microscopy: *syp-3(ok758)*, *syp-3(me42)*, and wild-type adult hermaphrodites (19 hr post-L4) were prepared for high pressure freezing as described in MacQueen *et al.* (2002). We analyzed 100-nm-thick longitudinal sections of two to three worms for every genotype for presence of SC in nuclei from transition zone through late pachytene stages.

RESULTS

SYP-3 is a coiled-coil protein required for proper synapsis and chiasma formation: *syp-3* was identified both through a genetic screen and an RNAi-mediated functional genomics screen for the identification of meiotic genes (see materials and methods). The former led to the identification of *syp-3(me42)*, which was mapped to within 0.5 cM of SNP pkP1059 on chromosome I. The latter identified F39H2.4, which upon depletion by RNAi elicited phenotypes similar to that of *syp-3* mutants (see below). Sequencing of *syp-3(me42)* indicated the presence of a nonsense mutation generating a stop codon at position 214 of the 224-amino acid protein encoded by F39H2.4 (Figure 1A). Therefore, *syp-3(me42)* encodes a C-terminal truncated form of SYP-3. Sequencing of a second *syp-3* mutation generated by the *Caenorhabditis* Gene Knockout Consortium, *syp-3(ok758)*, indicated that it carries a 1341-bp deletion encompassing the gene's promoter and 92% of its coding region (Figure 1A). Analysis of *syp-3(ok758)* through combined genetic, cytological, and molecular biology approaches (see materials and methods) indicates it is a null. BLAST searches revealed an ortholog of SYP-3 in *C. briggsae* but no other significant matches. Analysis utilizing the COILS and multicoil programs (Lupas *et al.* 1991; Wolf *et al.* 1997) revealed that SYP-3 carries predicted α-helical coiled-coils between residues 67 and 167.

Analysis of *syp-3* mutants revealed errors in chromosome segregation. This analysis relied on the basis for sex determination in *C. elegans* that consists of males (XO) and hermaphrodites (XX), where a self-fertilizing hermaphrodite lays mostly hermaphroditic progeny accompanied by a very low frequency of males (0.2%; Hodgkin *et al.* 1979). Mutations affecting chromosome segregation lead to increases in the frequency of male progeny (Him phenotype) and inviable aneuploid embryos laid

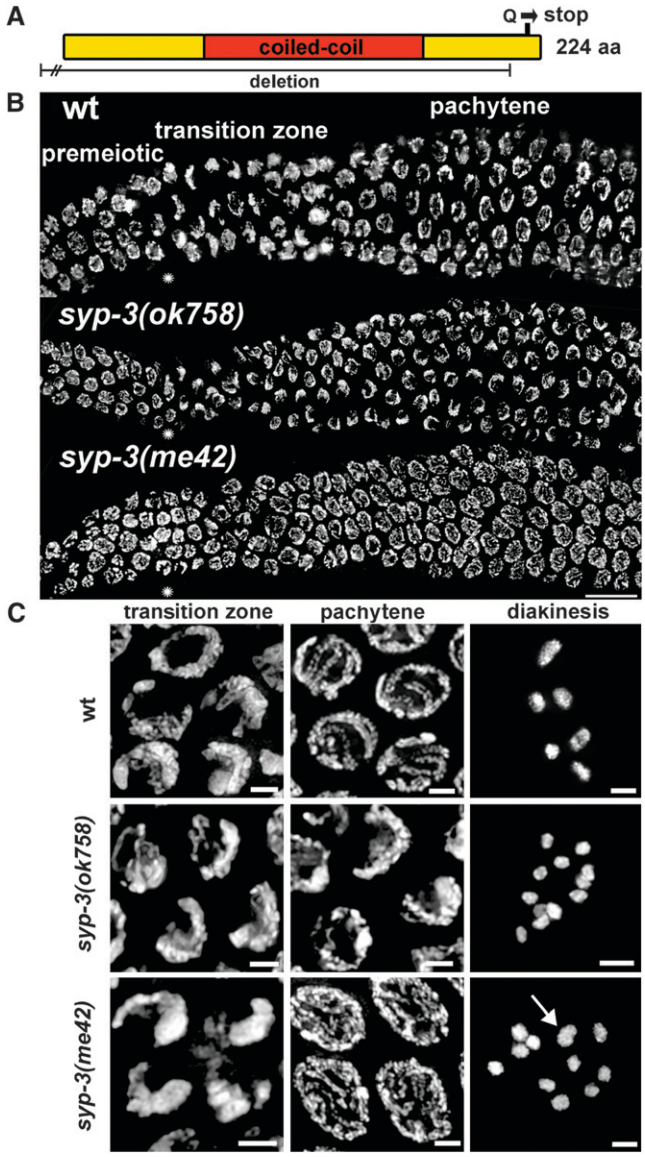

Figure 1.—SYP-3 is a coiled-coil protein required for normal chromosome morphogenesis and nuclear organization during meiotic prophase. (A) Schematic of the SYP-3 protein depicting the region deleted in *syp-3(ok758)* and the stop caused by the *syp-3(me42)* mutation. (B and C) Low and high magnification images, respectively, of DAPI-stained nuclei of whole-mount gonads from age-matched wild-type, *syp-3(ok758),* and *syp-3(me42)* adult hermaphrodites. Entrance into meiosis at the transition zone (leptotene/zygotene) is indicated by an asterisk in B. Arrow indicates two superimposed univalents in the *syp-3(me42)* diakinesis oocyte in C. Images in B and the first two columns in C are projections halfway through 3D data stacks of whole nuclei, while images in the last column of C encompass entire nuclei. Bar in B, 15 μm; bars in C, 2 μm.

by hermaphrodites. Both *syp-3* mutants had elevated levels of embryonic lethality [*syp-3(ok758)* = 96.4%, n = 2282; *syp-3(me42)* = 96.5%, n =1910] and a strong Him phenotype [*syp-3(ok758)* = 37% males; *syp-3(me42)* = 36% males].

Cytological examination of germline chromosome morphology in the *syp-3* mutants indicated that their chromosome segregation defect stems from the earlier role of SYP-3 in chromosome synapsis. Moreover, it also revealed phenotypic differences between the *syp-3* alleles. In both mutants, nuclei entered normally into the transition zone (leptotene/zygotene), with chromosomes acquiring the polarized spatial organization characteristic of this stage (Figure 1, B and C). However, in the *syp-3(ok758)* null mutant, chromosomes failed to redisperse as nuclei entered into the region corresponding to pachytene in wild type. Instead, chromosomes persisted in a transition zone-like organization for most of this region, redispersing only in nuclei very late in pachytene. Moreover, upon redispersal, instead of the thick and parallel DAPI-stained tracks characteristic of this stage for wild type, unsynapsed, thin chromatin tracks were apparent, similar to the appearance of the chromatin in *syp-1* and *syp-2* mutants (Figure 1, B and C). In contrast, in *syp-3(me42)* mutants, chromosomes redispersed prematurely throughout the nuclear periphery. Specifically, only 46.5% of wild-type levels of nuclei with a transition zone morphology were observed in this mutant allele. Redispersed chromosomes observed in nuclei throughout the pachytene region in *syp-3(me42)* were unsynapsed, forming instead unpaired and thin chromatin tracks. Finally, at diakinesis 12 univalents as opposed to 6 bivalents were observed in oocytes for both *syp-3* mutants, reflecting a lack of chiasmata (Figure 1C). This absence of chiasmata results from an inability to form crossovers, as we demonstrated in the accompanying article by Smolikov *et al.* (2007, this issue).

SYP-3 is a structural component of the SC: Immunolocalization of SYP-3 throughout meiotic prophase strongly supports its role as a structural component of the SC. SYP-3 is observed colocalizing with SYP-1 at bright foci present in the first few nuclei upon entrance into meiosis (Figure 2A). Since SYP-1 and SYP-2 also colocalize in these foci and throughout meiotic prophase (data not shown), by extension, the parallels made between SYP-1 and SYP-3 localization from this point onwards can be extrapolated to SYP-2 and SYP-3 as well. This initial colocalization at bright foci is followed by an extensive localization of SYP-3 along chromosomes during early to mid-transition zone, while chromosomes are still in the clustered organization characteristic of this stage. This is distinct from the localization pattern observed for either SYP-1 or SYP-2, which are restricted to short or discontinuous stretches along chromosomes until halfway between mid- and late transition zone (Figure 2B; MacQueen *et al.* 2002; Colaiácovo *et al.* 2003). However, short stretches of SYP-1 immunostaining were observed only along regions exhibiting extensive SYP-3 association. Upon entrance into pachytene, SYP-3 localizes continuously at the interface between paired and aligned homologous chromosomes, similarly to SYP-1 and SYP-2 (Figure 2C; MacQueen *et al.* 2002; Colaiácovo *et al.* 2003). As nuclei progress through late prophase and the SC disassembles, SYP-3 localization is the same

as that observed for SYP-1 and SYP-2 (Nabeshima *et al.* 2005). SYP-3 chromosomal association is progressively reduced, becoming restricted to the mid-bivalents in early diakinesis (supplemental Figure 1 at http://www.genetics.org/supplemental/), and is no longer apparent at the last oocyte prior to fertilization (Figure 2D).

The chromosomal association of SYP-3 perfectly parallels the timing of SC assembly and disassembly, suggesting it may act as a structural component of the SC. Interestingly, the staining pattern observed during transition zone resembles that previously reported for the axial component HIM-3 (Zetka *et al.* 1999). In contrast, the pattern of chromosomal dissociation resembles that of the central region components SYP-1 and SYP-2 and not HIM-3, which persists associated with chromosomes through the metaphase I to anaphase I transition (Zetka *et al.* 1999; MacQueen *et al.* 2002; Colaiácovo *et al.* 2003). This localization pattern suggests a role for SYP-3 in interconnecting two major units involved in SC assembly, the lateral elements and central region.

Transmission electron microscopy (TEM) further supports a role for SYP-3 in SC formation (Figure 2, E–G). In *syp-3(ok758)* and *syp-3(me42)* germline nuclei ($n = 169$ and $n = 160$, respectively) the SC was never detected, while in wild type, 94.7% of the germline nuclei ($n = 137$) carried between one and five SC stretches. Densely stained regions corresponding to chromatin usually acquired a parallel organization with a clear array of transverse filaments lying between them in wild-type germline nuclei. However, in the *syp-3* mutants, electron-dense chromatin was present but not associated with any detectable SCs.

SC central region formation, but not axis morphogenesis, is SYP-3 dependent: To further examine the role of SYP-3 in SC assembly, we examined the interdependencies between SYP-3 and both axis-associated and central region components of this structure (Figure 3). In both *syp-3* mutants, the chromosomal association of the lateral element component HIM-3 and the meiosis-specific cohesin REC-8 unfolded as in wild type with regard to both timing and specific localization (Figure 3, A–F). Both α-HIM-3 and α-REC-8 staining were observed on chromosomes upon entrance into the transition zone, forming continuous stretches along chromosomes at pachytene and remaining associated with chromosomes beyond late prophase.

In contrast, SYP-3 chromosomal localization was impaired in both *him-3(gk149)* (a null allele) and in *rec-8(RNAi)* worms (Figure 3, G and H). In *him-3(gk149),* just a single bright focus of SYP-3 staining was observed

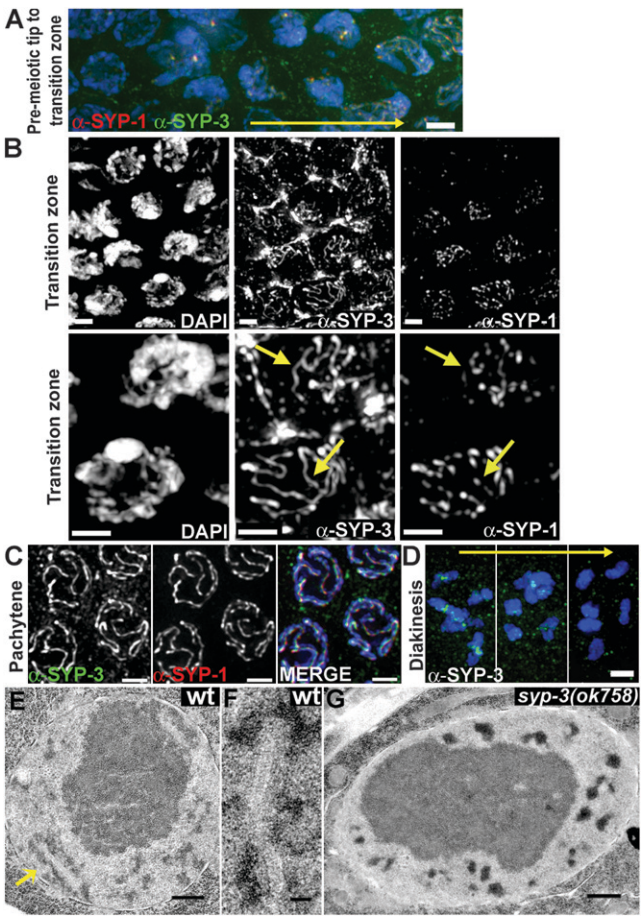

Figure 2.—Immunolocalization and TEM analysis place SYP-3 as a structural component of the SC. (A–D) Immunolocalization of SYP-3 throughout meiotic prophase. Images in A–C are projections halfway through 3D data stacks of whole nuclei; images in D encompass entire nuclei. DAPI-stained chromosomes are in blue in A, C, and D and in white in B. α-SYP-3 is in green in A, C, and D and in white in B. α-SYP-1 is in red in A and C and in white in B. (A) Progression into transition zone is observed from left to right in this field of nuclei, as indicated by the yellow arrow. SYP-3 is observed colocalizing with SYP-1 to discrete chromosomal foci in early transition zone. (B) Progression into transition zone is observed top to bottom in this field of nuclei. SYP-3 is observed localizing extensively throughout chromosomes by mid-transition zone. High magnification images of mid-transition zone nuclei indicate that SYP-3 chromosomal localization is more extensive at this stage compared to SYP-1 (indicated by yellow arrows). The hexagonal staining pattern observed corresponding to the cellular membrane is the nonspecific background also present in the *syp-3(ok758)* null mutant (Figure 4). (C) SYP-3 colocalizes with SYP-1 continuously at the interface between paired and aligned homologs during pachytene. (D) SYP-3 localization becomes restricted to the mid-bivalents at diakinesis and progressively dissociates from chromosomes, being no longer present at late diakinesis (progression is indicated by yellow arrow). (E–G) TEM images of mid-pachytene nuclei in wild-type and *syp-3(ok758)* germlines. (E) Equatorial section of a wild-type pachytene nucleus where the large dark body slightly off-center is the nucleolus surrounded by SC stretches (indicated by yellow arrow) visible as "zipper-like" structures flanked by electron-dense chromatin patches. (F) Higher magnification of an SC from a different wild-type nucleus. (G) In both *syp-3* mutants [exemplified here by *syp-3(ok758)*], chromatin patches are observed distributed around the nucleolus and SCs are absent. Bars in A–D, 2 μm; in E and G, 500 nm; in F, 100 nm.

associated with DAPI-stained chromosomes in nuclei throughout the transition zone and early pachytene. Throughout mid- and late pachytene nuclei, SYP-3 chromosomal localization consisted mostly of either up to two bright foci or a single short stretch per nucleus. These regions of residual SYP-3 staining coincided with the only regions stained by both α-SYP-1 and α-SYP-2 (data not shown). SYP-3 localization was no longer apparent throughout oocytes in diplotene and diakinesis. These results indicate that HIM-3 is required for SYP-3 assembly during meiotic prophase. In *rec-8(RNAi)* worms, chromosomal localization of SYP-3 was reduced but not fully eliminated, similar to SYP-2 (Colaiácovo *et al.* 2003). Various chromatin stretches lacking SYP-3 staining were apparent. This partial reduction in SYP-3 staining may be due to the partial depletion of REC-8 in the *rec-8(RNAi)* worms. Although only worms with oocytes carrying 24 univalents (indicative of separated sister chromatids as a result of depleting the meiotic specific cohesin; Pasierbek *et al.* 2001) were examined for SYP-3 staining, REC-8 antibody staining of these worms confirmed that depletion was only partial (data not shown). Altogether, these results indicate that while axis morphogenesis unfolds independently of SYP-3 function, SYP-3 requires both HIM-3 and REC-8 for its chromosomal localization.

While SYP-3 is not required for axis morphogenesis, it is required for the localization and stability of SC central region proteins SYP-1 and SYP-2. In *syp-3(ok758)*, neither SYP-1 nor SYP-2 localization was observed in nuclei throughout meiotic prophase (shown for SYP-1, Figure 3I) compared to wild type (Figure 3, J and M). Moreover, SYP-3 localization is interdependent with SYP-1 and SYP-2, as SYP-3 localization was no longer observed throughout meiotic prophase in both *syp-1* and *syp-2* null mutants (Figure 4).

Whereas the *syp-3* null mutant lacked SYP-1, SYP-2, and SYP-3 proteins in meiotic nuclei throughout prophase, the *syp-3* mutant with the C-terminal truncation of SYP-3 exhibited aberrant localization of SYP-1 throughout most of meiotic prophase. Upon entrance into transition zone in *syp-3(me42)* mutants, SYP-1 and SYP-2 surround chromosomes but do not directly associate along chromatin tracks (shown for SYP-1, Figure 3, J–L). This is not due to a general inaccessibility of chromatin to the association of SC components, given that HIM-3 and HTP-3 (a HIM-3 paralog associated with chromosome axes prior to chromosome pairing; MacQueen *et al.* 2005) localize with

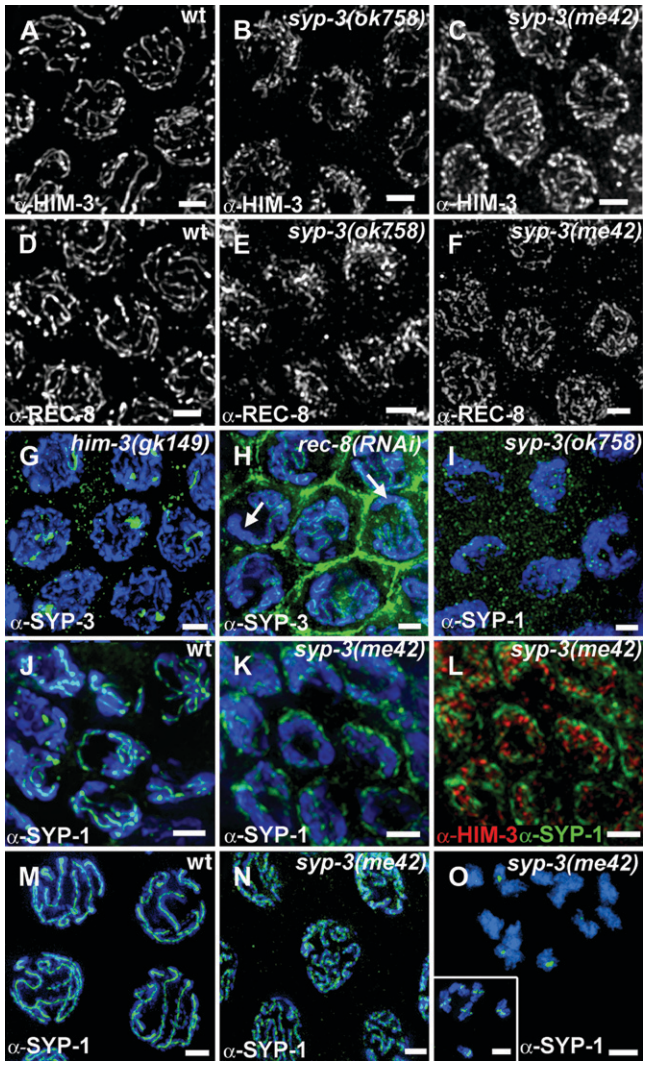

Figure 3.—SYP-3 acts downstream of axis morphogenesis and is required for central region formation. (A–F) Immunostaining with either α-HIM-3 or α-REC-8 of wild-type, *syp-3(ok758)*, and *syp-3(me42)* pachytene nuclei. DNA is not shown to facilitate the observation of continuous stretches of both HIM-3 and REC-8 (white) in all 3 genotypes, which is a clearly evident feature when looking at 3D image stacks but is slightly obscured in 2D projections, particularly of *syp-3(ok758)*, due to the persistent chromosome clustering characteristic of this mutant. (G and H) α-SYP-3 immunostaining (green) of *him-3(gk149)* and *rec-8(RNAi)* pachytene nuclei (DNA in blue). SYP-3 localization is impaired when axis morphogenesis is defective. In the *him-3* null allele, only short stretches or large foci of SYP-3 staining are observed, while in *rec-8(RNAi)*, SYP-3 staining is discontinuous as indicated by arrows. (I–O) Immunostaining of wild-type, *syp-3(ok758)*, and *syp-3(me42)* nuclei (DNA shown in blue) with either α-SYP-1 (green) or α-HIM-3 (red). (I) SC central region formation is impaired in *syp-3(ok758)* as indicated by the lack of α-SYP-1 staining in nuclei in the pachytene region. (J) α-SYP-1 stains continuously along wild-type chromosomes in mid- to late transition zone. (K and L) DAPI-stained chromosomes only with α-SYP-1 staining are shown separately (K) to facilitate the observation that during transition zone in *syp-3(me42)*, SYP-1 surrounds the clustered chromosomes and, unlike HIM-3, fails to localize directly onto chromosomes. (M and N) As a central region component of the SC, SYP-1 localizes at the interface between synapsed pachytene chromosomes in wild type. However, in *syp-3(me42)*, SYP-1 localizes along thin DAPI-stained tracks. (O) While SYP-1 is present only at the mid-section of all six bivalents in wild-type diakinesis oocytes (inset), it is observed on some univalents in *syp-3(me42)*. All immunostainings were performed on whole mounts of dissected germlines. Images in A–N are projections halfway through 3D data stacks of nuclei, while images in O encompass entire nuclei. Bars, 2 μm.

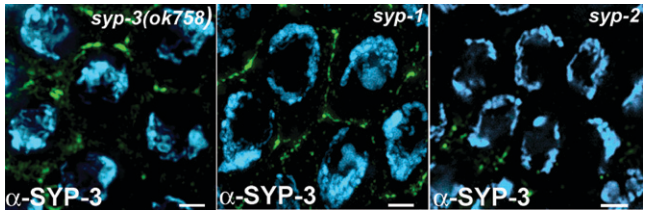

Figure 4.—SYP-3 chromosomal localization is dependent on SYP-1 and SYP-2. DAPI-stained mid-pachytene nuclei are in blue (projections are halfway through 3D data stacks). α-SYP-3 is in green. The hexagonal staining pattern observed corresponding to the cellular membrane is the nonspecific background also present in the *syp-3(ok758)* null mutant. Bars, 2 μm.

wild-type kinetics along these unsynapsed strands (Figure 3L and supplemental Figure 2 at http://www.genetics.org/supplemental/). The peripheral localization observed for SYP-1 and SYP-2 persists until entrance into pachytene when chromosomes redisperse. At this stage, both foci and short stretches of SYP-1 and SYP-2 localized throughout unsynapsed chromosomes (shown for SYP-1, Figure 3, M and N, and supplemental Figure 2). To examine this chromosomal association during pachytene in more detail, we compared SYP-1 localization in wild-type, *htp-1(me84)*, and *syp-3(me42)* squashed nuclei (Figure 5). SYP-1 localized continuously between either homologously or nonhomologously paired and synapsed chromosomes, respectively, in wild type and *htp-1(me84)*. This was indicated by the antibody signal flanked by DAPI signals on both sides. In contrast, in the *syp-3(me42)* mutant, SYP-1 formed both foci and short stretches, presumably both along and between sister chromatids, given that the antibody signal was both adjacent to single tracks of DAPI (indicated by arrowheads) or flanked by DAPI signals (indicated by thin arrows) that were narrower than those observed for synapsed chromosomes in either wild type or *htp-1(me84)*. Finally, chromosomal association of SYP-1 and SYP-2 is also observed on univalents during early diakinesis in *syp-3(me42)* mutants (Figure 3O). As in wild type, this association decreases throughout late prophase and is no longer observed by the last oocyte prior to sperm. Taken together, these results suggest a potential role for SYP-3 in regulating the specific association of the central region components of the SC such that it initiates at transition zone and occurs between homologs.

Interestingly, immunostaining of the *syp-3(me42)* mutant with α-SYP-3 antibody revealed residual SYP-3 staining (Figure 6). Specifically, we did not observe SYP-3 staining on chromosomes at the transition zone and observed only a weak and punctate staining along unsynapsed chromosomes in pachytene nuclei. This suggests either that the C-terminal truncation leads to reduced levels of SYP-3 protein or that the C terminus of SYP-3 may be required for its timely and precise association onto chromosomes during prophase. In either case, these observations further support a role for SYP-3 in regulating the proper loading of SYP-1 and SYP-2 at the transition zone.

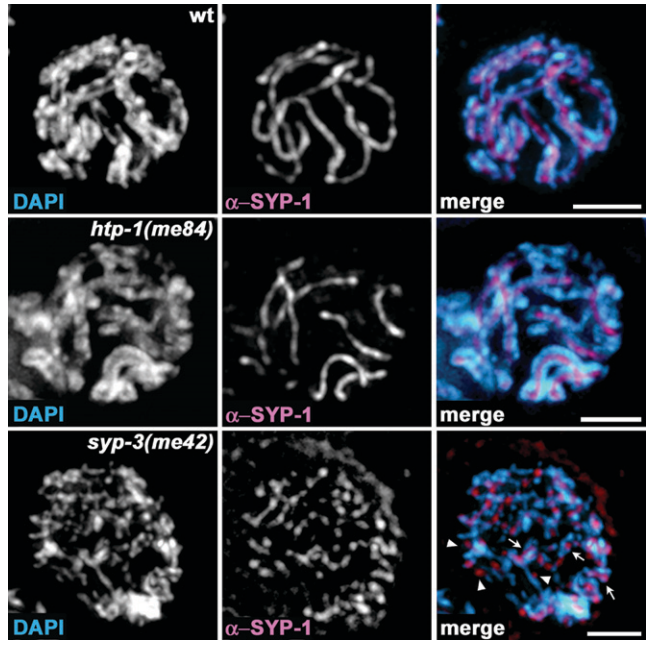

Figure 5.—SYP-3 is required to restrict SC assembly to bridge paired chromosome axes. Squash preparations of DAPI-stained pachytene nuclei of wild-type, *htp-1(me84)*, and *syp-3(me42)* mutants immunostained with α-SYP-1. Thick SYP-1 lines in wild-type and *htp-1(me84)* are flanked by parallel tracks of DAPI. In *syp-3(me42)*, foci and short stretches of SYP-1 are either located to one side of thin DAPI tracks (arrowheads) or flanked by thin DAPI signals (thin arrows). Images are projections halfway through 3D data stacks of nuclei. Bars, 2 μm.

SYP-3 is required for the stabilization of homologous pairing: Quantitative analysis of chromosomal pairing by FISH indicates a role for SYP-3 in the stabilization of pairing, as previously demonstrated for SYP-1 and SYP-2. We monitored pairing at five different chromosomal loci in the *syp-3* mutants, compared to *syp-1*, *syp-2*, and wild type, taking advantage of the temporal and spatial order in which nuclei are arranged within the germline. Pairing at opposite ends of an autosome (chromosome I), the X chromosome, as well as a more internal region (5S rDNA) of chromosome V, were compared (Figure 7).

In wild type, levels of homologous chromosome pairing progressively increase upon entrance into meiosis (transition zone, zones 2–3; Figure 7, A and B), and ~100% of the nuclei examined carry stably paired homologs throughout pachytene (zones 4–7). Moreover, 100% pairing is achieved both along autosomes and the X chromosome (this work; MacQueen *et al.* 2002). In the *syp-3* null, although some level of pairing was achieved upon entrance into prophase compared to basal pairing levels observed in the premeiotic tip (zone 1), overall pairing was significantly impaired. Specifically, in *syp-3(ok758)* mutants, the level of pairing observed throughout early prophase was comparable to that observed in

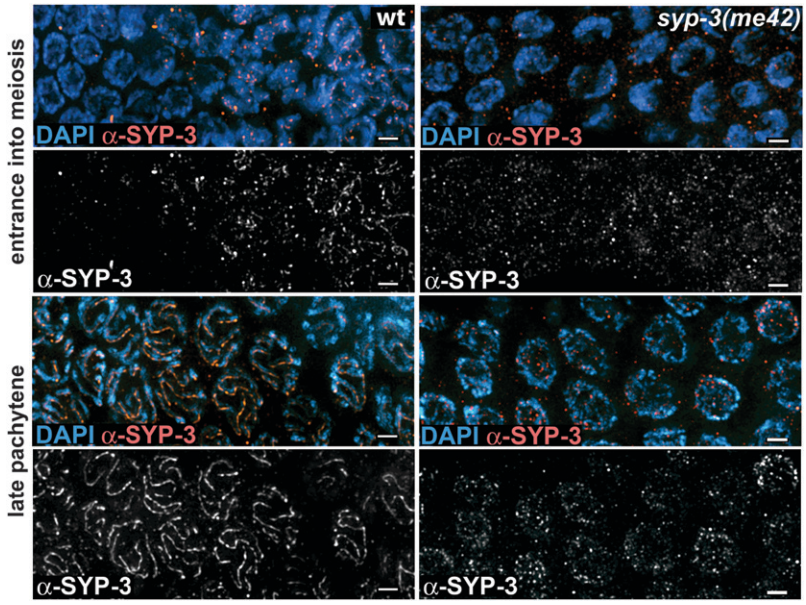

FIGURE 6.—Examining the effect of a C-terminal truncation of SYP-3 on its chromosomal localization. DAPI-stained chromosomes (blue) are immunostained with α-SYP-3 C-terminal antibody (red). Progression into the transition zone and through late pachytene is observed from left to right, respectively, on the top four and bottom four panels in wild type and *syp-3(me42)*. Projections are halfway through 3D data stacks. Bars, 2 μm.

syp-1 and *syp-2* mutants at the same stage. At the 5S rDNA locus on chromosome V, for example, only 16 and 46% of nuclei carried paired chromosomes in zones 2 and 3, respectively, compared to 23 and 84% in wild type. Moreover, these pairing frequencies were not maintained throughout pachytene, implicating SYP-3 in the stabilization of homologous pairing together with SYP-1 and SYP-2.

Comparisons between the PC and non-PC ends of chromosomes revealed that the overall frequencies of homologous pairing were higher in the PC as opposed to the non-PC ends in the *syp-3* null. Specifically, the

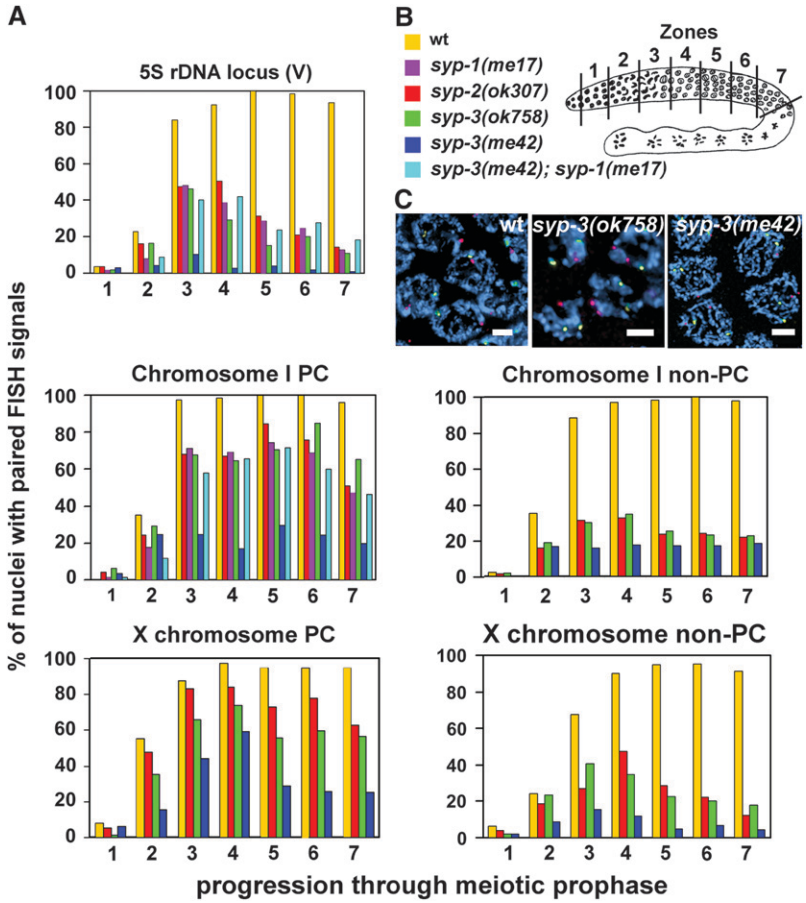

FIGURE 7.—Homologous pairing is impaired in *syp-3* mutants. (A) Graphs depict the percentage of nuclei carrying paired homologs (*y*-axis) within each zone along the germline (*x*-axis). The regions being probed are specified above each graph. The color-coded columns represent the various genotypes examined. (B) Germline diagram indicates the position of the zones scored for time-course analysis of homologous pairing. (C) Pachytene nuclei of whole mounts hybridized with FISH probes recognizing the 5S rDNA locus (green) and the X chromosome PC end (red). Signals are not paired in most nuclei in *syp-3* mutants compared to wild type, where a single focus or closely juxtaposed foci are apparent for both probes in each nucleus. Bars, 2 μm.

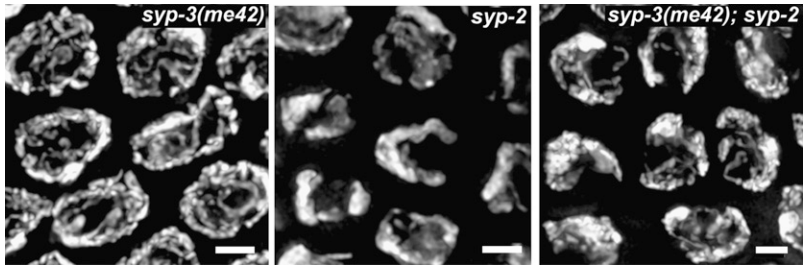

FIGURE 8.—Examining how changes in chromosome structure affect their spatial organization. DAPI-stained nuclei at mid-pachytene (projections are halfway through 3D data stacks) are depicted. In *syp-3(me42); syp-2* mutants, chromosomes no longer redisperse prematurely as in *syp-3(me42)*. Instead, they persist in a polarized nuclear organization as in *syp-2* single mutants. Bars, 2 μm.

maximum pairing levels achieved in *syp-3(ok758)* mutants were on average 1.7-fold higher at the PC compared to the non-PC ends of chromosomes. This observation indicates that PC end-mediated pairing is less dependent on SYP-3 than pairing along non-PC regions.

Interestingly, pairing was more severely impaired in *syp-3(me42)* mutants than in the *syp-3* null mutants for all five loci tested. During early prophase at the 5S rDNA locus on chromosome V, for example, there were four- to fivefold fewer nuclei carrying paired homologs in *syp-3(me42)* compared to the *syp-3* null. In addition, as described earlier, a relatively shorter transition zone is observed in *syp-3(me42)* and chromosomal association of SYP-1 and SYP-2 still occurs, albeit not coupling the axes of homologous chromosomes. Taken together, these observations suggest that the inappropriate association of SYP-1 and SYP-2 might be responsible for the premature redispersal of chromosomes and/or the lower incidence of pairing in the *syp-3(me42)* mutants. We tested this possibility by examining pairing levels in *syp-3(me42); syp-1* double mutants (Figure 7) and chromosome organization in both *syp-3(me42); syp-1* and syp-*3(me42); syp-2* double mutants (only the latter is shown in Figure 8). In *syp-3(me42); syp-1* mutants, maximum pairing levels observed both at the PC end of chromosome I and at the 5S rDNA region of chromosome V were improved compared to *syp-3(me42),* reaching levels comparable to that of *syp-1* mutants (72 and 42%, respectively). Further, both this double mutant and *syp-3(me42); syp-2* exhibited prolonged persistence of chromosomes in a polarized nuclear organization, as observed in *syp-1*, *syp-2*, and *syp-3* null single mutants. Together, these observations suggest that SYP-1 and SYP-2 loading onto chromosome axes in the *syp-3(me42)* mutant may indeed interfere with homologous pairing, possibly by leading to a premature exit from a polarized nuclear organization and thereby reducing the duration of the stage during which pairing can be achieved.

DISCUSSION

Structural and regulatory roles for SYP-3 in promoting SC formation between paired homologs: Several observations indicate that SYP-3 is a structural component of the SC. First, immunolocalization of SYP-3 places it at the interface between paired and aligned homologous chromosomes. Second, TEM analysis further supports the conclusion that SYP-3 is required for chromosome synapsis throughout prophase. Third, analysis of SYP-3 interdependencies for chromosomal association indicate it acts downstream of axis morphogenesis and is required for SC central region formation. More specifically, immunolocalization of SYP-1, SYP-2, and SYP-3 in synapsis-defective mutants, including the *syp-3* null, indicate that SYP-1, SYP-2, and SYP-3 are required for each other's association onto chromosomes. Although the SYP proteins are interdependent for and largely identical in their chromosomal localization through most of prophase, several observations raise the possibility that SYP-3 may have roles that distinguish it from either SYP-1 or SYP-2. First, immunolocalization experiments suggest that SYP-3 polymerizes more extensively between homologous chromosomes in early transition zone, followed by SYP-1 and SYP-2, although we cannot rule out the possibility that this distinction may be a result of differences in antibody affinities and/or epitope accessibility. Further, analysis of *syp-3(me42)* suggests that SYP-3 plays a role in restricting the association of central region components at early prophase to occur only in an appropriate context, coupling the axes of paired homologous chromosomes.

The extensive localization of SYP-1 and SYP-2 along unsynapsed chromosomes is one of the most striking features of the *syp-3(me42)* mutant phenotype, as loading of SC central region proteins normally occurs only between paired homologs. Moreover, this phenotype is distinct from the nonhomologous synapsis observed previously in *htp-1* null mutants and *him-3* hypomorphs in *C. elegans*, where extensive SC polymerization occurs between the axes of nonhomologous chromosomes (COUTEAU *et al.* 2004; NABESHIMA *et al.* 2004; COUTEAU and ZETKA 2005; MARTINEZ-PEREZ and VILLENEUVE 2005). The observation of extensive association of SC central region proteins along the axes of isolated chromosomes emphasizes the need for an additional level of control governing SC assembly: not only must these proteins be prevented from bridging the axes of inappropriate partner chromosomes, but also they must be prevented from associating with isolated axes *per se*. While we cannot exclude the possibility that the aberrant loading of SYP-1 and SYP-2 in the *syp-3(me42)* mutant might be caused by reduced levels of SYP-3, we favor the idea that the C-terminal truncated protein has a capacity to stabilize

SYP-1 and SYP-2 and allow their association with chromosomes but lacks the capacity to prevent their association with the axes of unpaired chromosomes.

Triggering of chromosome dispersal by loading of SC components and its implications for pairing: The different features of chromosome organization observed in the *syp-3(ok758)* null and *syp-3(me42)* C-terminus truncated mutants enabled us to probe relationships between pairing, synapsis, and chromosome organization within the nucleus. First, they provide insight into the nature of the signal that promotes redispersal of chromosomes from the clustered configuration. Previous work has shown that loss of SC central region proteins results in persistence of chromosomes in a clustered organization throughout most of pachytene, indicating a role for SC central region assembly in promoting exit from a clustered organization (MacQueen *et al.* 2002; Colaiácovo *et al.* 2003). This finding is recapitulated here in our analysis of the *syp-3* null mutant. Further, recent work has suggested that this coupling is regulatory in nature, leading to the proposal that a checkpoint-like mechanism coordinates progression of homolog synapsis with chromosome redispersal in *C. elegans* (Martinez-Perez and Villeneuve 2005). According to this model, loading of SC central region components between paired homologs would serve to trigger chromosome dispersal by eliminating a "wait dispersal" signal analogous to the "wait anaphase" signal generated by unattached kinetochores in the spindle assembly checkpoint. Our finding that in *syp-3(me42)* mutants, chromosomes exit a clustered organization when loading of the SYP proteins occurs, suggests that the association of the SYP proteins, even if along unpaired chromosomes and not resulting in the coupling of homologous axes, may be capable of serving as a trigger leading to the release from a polarized chromosome organization.

The differences between the pairing profiles of the *syp-3* null and *syp-3(me42)* mutants also provide insight into the relationship between chromosome clustering and the active search for homologs during meiotic prophase. The pairing profile of the *syp-3* null mutant closely parallels those of *syp-1* and *syp-2* null mutants (MacQueen *et al.* 2002; Colaiácovo *et al.* 2003). In all three cases, chromosomal loci are able to achieve substantial levels of pairing but are unable to maintain these levels. This profile indicates that SYP-3 functions together with SYP-1 and SYP-2 to stabilize associations between homologs, acting downstream of PCs, which mediate local stabilization of homolog pairing even in the absence of synapsis (MacQueen *et al.* 2002, 2005). Interestingly, homologous pairing is more severely impaired in *syp-3(me42)* than in *syp-3(ok758).* Moreover, this reduction in pairing is alleviated in *syp-3(me42); syp-2* double mutants, strongly suggesting that loading of SC central region proteins is the cause of the severe pairing defect. These results could be interpreted to mean that inappropriate loading of central region proteins *per se* interferes directly with the homolog recognition process. However, these results must be interpreted in the context of the observation that *syp-3(me42)* mutants exhibit a premature exit from the clustered chromosomal organization, and this premature dispersal is also alleviated in *syp-3(me42); syp-2* double mutants, which exhibit persistent chromosome clustering. Together, these results suggest that exit from a polarized nuclear organization terminates chromosomal attempts to pair even though chromosomes have not yet established normal interhomolog interactions.

Premature exit from a polarized nuclear organization has also been observed in *htp-1* mutants, which are defective in autosomal pairing yet exhibit extensive synapsis between nonhomologous chromosomes (Couteau and Zetka 2005; Martinez-Perez and Villeneuve 2005). However, in contrast to *syp-3(me42); syp-2* double mutants, premature redispersal still occurred in *htp-1; syp-2* mutants (Martinez-Perez and Villeneuve 2005). We reconcile these observations by proposing that whereas the postulated checkpoint-like mechanism that coordinates progression of pairing and synapsis with chromosome redispersal is missing in *htp-1* mutants, the checkpoint is still functional in the *syp-3(me42)* mutant, with the association of SYP-1 and SYP-2 with chromosome axes being perceived as a signal to proceed with redispersal (as discussed above).

Taken together, our observations strengthen the association between chromosome clustering and the active search for homology and support the notion that successful synapsis triggers exit from this stage and progression into mid-prophase.

Some strains and clones were kindly provided by the *Caenorhabditis* Genetics Center, the *Caenorhabditis* Gene Knockout Consortium, the Sanger Center, Enrique Martinez-Perez, and Kentaro Nabeshima. We thank Monique Zetka for the HIM-3 and HTP-3 antibodies. We also thank Fred Winston and members of the Colaiácovo laboratory for critical reading of this manuscript. This work was supported in part by research grant no. 5-FY05-1214 from the March of Dimes Birth Defects Foundation and by National Institutes of Health grant R01GM072551 to M.P.C.; a DFG postdoctoral research fellowship PR1057/1-1 to K.S.-P.; and National Institutes of Health grant R01GM53804 to A.M.V.

LITERATURE CITED

Brenner, S., 1974 The genetics of *Caenorhabditis elegans.* Genetics **77:** 71–94.

Chikashige, Y., C. Tsutsumi, M. Yamane, K. Okamasa, T. Haraguchi *et al.*, 2006 Meiotic proteins bqt1 and bqt2 tether telomeres to form the bouquet arrangement of chromosomes. Cell **125:** 59–69.

Chua, P. R., and G. S. Roeder, 1997 Tam1, a telomere-associated meiotic protein, functions in chromosome synapsis and crossover interference. Genes Dev. **11:** 1786–1800.

Colaiácovo, M. P., 2006 The many facets of SC function during *C. elegans* meiosis. Chromosoma **115:** 195–211.

Colaiácovo, M. P., G. M. Stanfield, K. C. Reddy, V. Reinke, S. K. Kim *et al.*, 2002 A targeted RNAi screen for genes involved in chromosome morphogenesis and nuclear organization in the *Caenorhabditis elegans* germline. Genetics **162:** 113–128.

Colaiácovo, M. P., A. J. MacQueen, E. Martinez-Perez, K. McDonald, A. Adamo *et al.*, 2003 Synaptonemal complex assembly in *C. elegans* is dispensable for loading strand-exchange proteins but critical for proper completion of recombination. Dev. Cell **5:** 463–474.

Conrad, M. N., A. M. Dominguez and M. E. Dresser, 1997 Ndj1p, a meiotic telomere protein required for normal chromosome synapsis and segregation in yeast. Science **276:** 1252–1255.

Cooper, J. P., Y. Watanabe and P. Nurse, 1998 Fission yeast Taz1 protein is required for meiotic telomere clustering and recombination. Nature **392:** 828–831.

Couteau, F., and M. Zetka, 2005 HTP-1 coordinates synaptonemal complex assembly with homolog alignment during meiosis in *C. elegans*. Genes Dev. **19:** 2744–2756.

Couteau, F., K. Nabeshima, A. Villeneuve and M. Zetka, 2004 A component of *C. elegans* meiotic chromosome axes at the interface of homolog alignment, synapsis, nuclear reorganization, and recombination. Curr. Biol. **14:** 585–592.

Dernburg, A. F., K. McDonald, G. Moulder, R. Barstead, M. Dresser *et al.*, 1998 Meiotic recombination in *C. elegans* initiates by a conserved mechanism and is dispensable for homologous chromosome synapsis. Cell **94:** 387–398.

Ding, D. Q., A. Yamamoto, T. Haraguchi and Y. Hiraoka, 2004 Dynamics of homologous chromosome pairing during meiotic prophase in fission yeast. Dev. Cell **6:** 329–341.

Gerton, J. L., and R. S. Hawley, 2005 Homologous chromosome interactions in meiosis: diversity amidst conservation. Nat. Rev. Genet. **6:** 477–487.

Golubovskaya, I. N., L. C. Harper, W. P. Pawlowski, D. Schichnes and W. Z. Cande, 2002 The pam1 gene is required for meiotic bouquet formation and efficient homologous synapsis in maize (*Zea mays* L.). Genetics **162:** 1979–1993.

Harper, L., I. Golubovskaya and W. Z. Cande, 2004 A bouquet of chromosomes. J. Cell Sci. **117:** 4025–4032.

Hodgkin, J., H. R. Horvitz and S. Brenner, 1979 Nondisjunction mutants of the nematode *Caenorhabditis elegans*. Genetics **91:** 67–94.

Kelly, K. O., A. F. Dernburg, G. M. Stanfield and A. M. Villeneuve, 2000 *Caenorhabditis elegans msh-5* is required for both normal and radiation-induced meiotic crossing over but not for completion of meiosis. Genetics **156:** 617–630.

Lupas, A., M. Van Dyke and J. Stock, 1991 Predicting coiled coils from protein sequences. Science **252:** 1162–1164.

MacQueen, A. J., and A. M. Villeneuve, 2001 Nuclear reorganization and homologous chromosome pairing during meiotic prophase require *C. elegans chk-2*. Genes Dev. **15:** 1674–1687.

MacQueen, A. J., M. P. Colaiácovo, K. McDonald and A. M. Villeneuve, 2002 Synapsis-dependent and -independent mechanisms stabilize homolog pairing during meiotic prophase in *C. elegans*. Genes Dev. **16:** 2428–2442.

MacQueen, A. J., C. M. Phillips, N. Bhalla, P. Weiser, A. M. Villeneuve *et al.*, 2005 Chromosome sites play dual roles to establish homologous synapsis during meiosis in *C. elegans*. Cell **123:** 1037–1050.

Martinez-Perez, E., and A. M. Villeneuve, 2005 HTP-1-dependent constraints coordinate homolog pairing and synapsis and promote chiasma formation during *C. elegans* meiosis. Genes Dev. **19:** 2727–2743.

McKim, K. S., A. M. Howell and A. M. Rose, 1988 The effects of translocations on recombination frequency in *Caenorhabditis elegans*. Genetics **120:** 987–1001.

McKim, K. S., B. L. Green-Marroquin, J. J. Sekelsky, G. Chin, C. Steinberg *et al.*, 1998 Meiotic synapsis in the absence of recombination. Science **279:** 876–878.

Nabeshima, K., A. M. Villeneuve and K. J. Hillers, 2004 Chromosome-wide regulation of meiotic crossover formation in *Caenorhabditis elegans* requires properly assembled chromosome axes. Genetics **168:** 1275–1292.

Nabeshima, K., A. M. Villeneuve and M. P. Colaiácovo, 2005 Crossing over is coupled to late meiotic prophase bivalent differentiation through asymmetric disassembly of the SC. J. Cell Biol. **168:** 683–689.

Nimmo, E. R., A. L. Pidoux, P. E. Perry and R. C. Allshire, 1998 Defective meiosis in telomere-silencing mutants of *Schizosaccharomyces pombe*. Nature **392:** 825–828.

Page, S. L., and R. S. Hawley, 2003 Chromosome choreography: the meiotic ballet. Science **301:** 785–789.

Page, S. L., and R. S. Hawley, 2004 The genetics and molecular biology of the synaptonemal complex. Annu. Rev. Cell. Dev. Biol. **20:** 525–558.

Pandita, T. K., C. H. Westphal, M. Anger, S. G. Sawant, C. R. Geard *et al.*, 1999 Atm inactivation results in aberrant telomere clustering during meiotic prophase. Mol. Cell. Biol. **19:** 5096–5105.

Pasierbek, P., M. Jantsch, M. Melcher, A. Schleiffer, D. Schweizer *et al.*, 2001 A *Caenorhabditis elegans* cohesion protein with functions in meiotic chromosome pairing and disjunction. Genes Dev. **15:** 1349–1360.

Phillips, C. M., and A. F. Dernburg, 2006 A family of zinc-finger proteins is required for chromosome-specific pairing and synapsis during meiosis in *C. elegans*. Dev. Cell **11:** 817–829.

Phillips, C. M., C. Wong, N. Bhalla, P. M. Carlton, P. Weiser *et al.*, 2005 HIM-8 binds to the X chromosome pairing center and mediates chromosome-specific meiotic synapsis. Cell **123:** 1051–1063.

Reinke, V., H. E. Smith, J. Nance, J. Wang, C. Van Doren *et al.*, 2000 A global profile of germline gene expression in *C. elegans*. Mol. Cell **6:** 605–616.

Riddle, D. L., T. Blumenthal, B. J. Meyer and J. R. Priess, 1997 *C. elegans II*. Cold Spring Harbor Laboratory Press, Cold Spring Harbor, NY.

Rogers, E., J. D. Bishop, J. A. Waddle, J. M. Schumacher and R. Lin, 2002 The aurora kinase AIR-2 functions in the release of chromosome cohesion in *Caenorhabditis elegans* meiosis. J. Cell. Biol. **157:** 219–229.

Scherthan, H., 2001 A bouquet makes ends meet. Nat. Rev. Mol. Cell. Biol. **2:** 621–627.

Scherthan, H., M. Jerratsch, B. Li, S. Smith, M. Hulten *et al.*, 2000 Mammalian meiotic telomeres: protein composition and redistribution in relation to nuclear pores. Mol. Biol. Cell **11:** 4189–4203.

Smolikov, S., A. Eizinger, A. Hurlburt, E. Rogers and A. M. Villeneuve *et al.*, 2007 Synapsis-defective mutants reveal a correlation between chromosome conformation and the mode of double-strand break repair during *Caenorhabditis elegans* meiosis. Genetics **176:** 2027–2033.

Trelles-Sticken, E., J. Loidl and H. Scherthan, 1999 Bouquet formation in budding yeast: initiation of recombination is not required for meiotic telomere clustering. J. Cell Sci. **112**(Pt 5): 651–658.

Trelles-Sticken, E., M. E. Dresser and H. Scherthan, 2000 Meiotic telomere protein Ndj1p is required for meiosis-specific telomere distribution, bouquet formation and efficient homologue pairing. J. Cell Biol. **151:** 95–106.

Villeneuve, A. M., 1994 A cis-acting locus that promotes crossing over between X chromosomes in *Caenorhabditis elegans*. Genetics **136:** 887–902.

Wicks, S. R., R. T. Yeh, W. R. Gish, R. H. Waterston and R. H. Plasterk, 2001 Rapid gene mapping in *Caenorhabditis elegans* using a high density polymorphism map. Nat. Genet. **28:** 160–164.

Wolf, E., P. S. Kim and B. Berger, 1997 MultiCoil: a program for predicting two- and three-stranded coiled coils. Protein Sci. **6:** 1179–1189.

Zalevsky, J., A. J. MacQueen, J. B. Duffy, K. J. Kemphues and A. M. Villeneuve, 1999 Crossing over during *Caenorhabditis elegans* meiosis requires a conserved MutS-based pathway that is partially dispensable in budding yeast. Genetics **153:** 1271–1283.

Zetka, M. C., I. Kawasaki, S. Strome and F. Muller, 1999 Synapsis and chiasma formation in *Caenorhabditis elegans* require HIM-3, a meiotic chromosome core component that functions in chromosome segregation. Genes Dev. **13:** 2258–2270.

Zickler, D., and N. Kleckner, 1998 The leptotene-zygotene transition of meiosis. Annu. Rev. Genet. **32:** 619–697.

Zickler, D., and N. Kleckner, 1999 Meiotic chromosomes: integrating structure and function. Annu. Rev. Genet. **33:** 603–754.

Communicating editor: R. S. Hawley